

DEVELOPMENT AND CHARACTERIZATION OF A CAPILLARY  
ELECTROPHORESIS INSTRUMENT WITH LASER-INDUCED  
FLUORESCENCE DETECTION FOR ON-LINE MONITORING OF GLUTAMATE  
IN VIVO VIA MICRODIALYSIS

By

Kristian Edward Swearingen

RECOMMENDED:

Kelly Ann

Brian Rasley

Thomas K. Reer

Advisory Committee Chair

Sam Claus

Chair, Department of Chemistry & Biochemistry

APPROVED:

Dan Bonadonna

Dean, College of Natural Science and Mathematics

Susan M. Henneke

Dean of the Graduate School

December 13, 2005

Date

DEVELOPMENT AND CHARACTERIZATION OF A CAPILLARY  
ELECTROPHORESIS INSTRUMENT WITH LASER-INDUCED  
FLUORESCENCE DETECTION FOR ON-LINE MONITORING OF GLUTAMATE  
*IN VIVO* VIA MICRODIALYSIS

A THESIS

Presented to the Faculty  
Of the University of Alaska Fairbanks

in Partial Fulfillment of the Requirements  
for the Degree of

MASTER OF SCIENCE

By

Kristian Edward Swearingen, B.S.

Fairbanks, Alaska

December 2005

BIOSCI  
TP  
248.25  
C37  
S94  
2005

**BIOSCIENCES LIBRARY-UAF**



### Abstract

To elucidate the roles of key neurochemicals in the metabolic suppression of Arctic ground squirrels, a technique is required that is capable of on-line, *in vivo*, high temporal resolution, quantitative detection of neurotransmitters. A capillary electrophoresis instrument has been built that is coupled to microdialysis by flow-gated injection. Primary amines recovered *in vivo* via microdialysis are derivatized on-column by cyanide-catalyzed formation of fluorescent isoindoles with naphthalene-2,3-dialdehyde for laser-induced fluorescence detection. The system is capable of detecting base-line glutamate *in vivo* in 15-second intervals.

## Table of Contents

	Page
Signature Page.....	i
Title Page.....	ii
Abstract.....	iii
Table of Contents.....	iv
List of Figures.....	vi
Glossary of Abbreviations.....	vii
<b>Chapter 1 Introduction</b>	
1.1 Biological Hypothesis Development.....	1
1.1.1 Why Study Hibernation?.....	1
1.1.2 The Suprachiasmatic Nucleus and Hibernation.....	2
1.1.3 Key Neurotransmitters.....	3
1.1.4 Proposed Neurochemical Model.....	4
1.2 Technique Requirements.....	4
1.3 Microdialysis.....	5
1.4 Capillary Electrophoresis.....	5
<b>Chapter 2 Methods</b>	
2.1 Instrument.....	9
2.1.1 Microdialysis Probe Construction.....	10
2.1.2 Derivatization.....	11
2.1.3 Injection.....	12



2.1.4	Separation.....	13
2.1.5	Detection.....	14
2.2	Data Collection and Analysis.....	15
2.2.1	Data Acquisition.....	16
2.2.2	Data Viewer.....	17
2.2.3	Peak Integrator.....	18
2.3	Calibration.....	19
2.4	<i>In Vivo</i> Methods.....	19
<b>Chapter 3 Data</b>		
3.1	Probe Characterization.....	20
3.2	Calibration Data.....	21
3.3	<i>In Vivo</i> Data.....	22
<b>Chapter 4 Discussion</b>		
4.1	Analysis of the Technique.....	24
4.2	Future work.....	25
<b>References.....</b>		<b>27</b>

## List of Figures

	Page
Figure 1.1 A drop in heart rate (HR) precedes cooling of body temperature....	1
Figure 1.2 Side view of a conditioned electrophoresis capillary.....	6
Figure 1.3 Separation of charged particles in capillary electrophoresis.....	8
Figure 2.1 Schematic of the CE/LIF system.....	9
Figure 2.2 The tip of one of the microdialysis probes built in our laboratory...	10
Figure 2.3 A fully assembled microdialysis probe.....	10
Figure 2.4 The derivatization reaction.....	11
Figure 2.5 The flow-gated injection T.....	12
Figure 2.6 The mounted separation capillary.....	15
Figure 2.7 The instrument control and data acquisition screen .....	16
Figure 2.8 The data viewer screen.....	17
Figure 2.9 The peak integrator screen.....	18
Figure 3.1 A discrete change in glutamate concentration.....	20
Figure 3.2 Calibration data for glutamate.....	21
Figure 3.3 A calibration curve.....	22
Figure 3.4 Detail of an <i>in vivo</i> electropherogram.....	23



### Glossary of Abbreviations

aCSF	artificial cerebrospinal fluid
AGS	arctic ground squirrel
CE	capillary electrophoresis
CE/LIFD	capillary electrophoresis with laser-induced fluorescence detection
CNS	central nervous system
DAQ	data acquisition
EOF	electroendosmotic flow
GABA	$\gamma$ -aminobutyric acid
HPLC	high performance liquid chromatography
NDA	naphthalene-2,3-dicarboxaldehyde
NMDA	N-methyl-D-aspartate
NMR	nuclear magnetic resonance spectroscopy
PMT	photomultiplier tube
RDGU	relative 2-deoxy-D-glucose uptake
SCN	suprachiasmatic nucleus

## Chapter 1 Introduction

### 1.1 Biological Hypothesis Development

#### 1.1.1 Why Study Hibernation?

Mammalian hibernation is of great interest to a number of researchers. Besides being intrinsically fascinating, the remarkable adaptations exhibited by hibernators - resistance to ischemia, hypoxia, and necrosis from tissue trauma, among other things - have the potential to be of great benefit to human health (Drew et al., 2001).

It is most likely that metabolic suppression in hibernators is controlled by the central nervous system (CNS). Figure 1 shows the heart rate (HR) and body temperature (Tb) of an arctic ground squirrel (AGS) entering hibernation. Taking

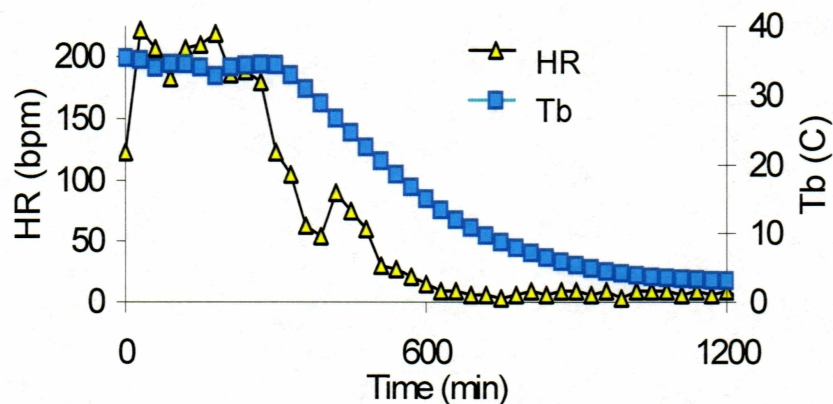


Figure 1.1 A drop in heart rate (HR) precedes cooling of body temperature (Tb) in an Arctic ground squirrel entering hibernation. Figure courtesy Kelly Drew.



HR as an indicator of metabolic activity, a precipitous drop in metabolic activity is seen followed by a passive cooling of the body to the ambient temperature of 2 degrees C. If the metabolic suppression observed in AGS were the effect of hypothermia, HR and Tb would be expected to drop concomitantly. That the metabolism drops first suggests that the homeostatic thermal set point is in essence reset, and that the body passively cools to this new set point. Since homeostatic set points are regulated by the CNS, it is believed that hibernation must also be regulated by the CNS.

#### 1.1.2 The Suprachiasmatic Nucleus and Hibernation

The suprachiasmatic nucleus (SCN) of the hypothalamus is well known to be the “master clock” for circadian rhythm. Located directly above the optic chiasm (the point at which the optic nerves from each eye decussate before proceeding to the optic area), it is directly involved in photoentrainment to day/night cycles by glutamatergic signals from the retina via the retinohypothalamic pathway. The SCN's involvement in circadian rhythms suggests that it may be involved in certain circannual rhythms as well. Lesioning of the SCN in hibernating ground squirrels drastically affects hibernation patterns (Ruby et al., 1996).

During torpor, a time when protein synthesis in the brain essentially shuts down, the SCN exhibits relatively high protein synthesis (Drew et al. preliminary

data), suggesting that it remains active during hibernation. Kilduff et al. (1989) have shown that relative 2-deoxy-D-glucose uptake (RDGU) in the SCN actually increases as a ground squirrel enters hibernation, reaching a maximum at the depth of torpor, then decreases as the animal emerges from torpor. That SCN activity increases during hibernation makes it a prime candidate for study of the regulation of metabolic suppression.

### 1.1.3 Key Neurotransmitters

If the SCN is involved in suppression of metabolism, one should expect to see an increase in the activity of inhibitory neurotransmitters in the SCN or in neural pathways efferent from the SCN. Nurnberger et al. (2000) have shown by immunocytochemistry that levels of  $\gamma$ -aminobutyric acid (GABA, an inhibitory neurotransmitter) remain high in the SCN during torpor. In addition to this, an excitatory neurotransmitter is also at work. Sibson et al. (1998) have demonstrated by *in vivo* C-13 NMR that RDGU is stoichiometrically linked to glutamate release. This means that the RDGU in the SCN of hibernating ground squirrels observed by Kilduff et al. directly correlates to glutamate release. Harris et al. (2000) have found that administration of MK-801, an N-methyl-D-aspartate (NMDA, a class of glutamate receptor) antagonist, causes arousal in hibernating golden mantled ground squirrels, further suggesting that glutamate is involved in active suppression of metabolism during hibernation.



#### 1.1.4 Proposed Neurochemical Model

Given the above data, the following hypothesis has been proposed: hibernation is initiated and maintained, at least in part, by GABAergic neurons efferent from the SCN. These GABAergic neurons are activated by glutamatergic interneurons. If this is the case, then the extracellular concentration of glutamate in the SCN can be expected to increase with immergence into torpor and decrease with emergence from torpor.

#### 1.2 Technique Requirements

In order to test the above-describe hypothesis, a technique was needed with the following capabilities: 1) the technique would need to be capable of detecting glutamate in the brain (as an indicator of glutamate release) at the concentrations observed *in vivo*, and of distinguishing glutamate from other neurotransmitters present; 2) the technique would need to be able to reflect changing levels of glutamate throughout the hibernation cycle; 3) the technique would need to be capable of collecting data points in fairly rapid succession so that no potentially important change in glutamate concentration would be missed; and 4) the technique would need to be able to do all of this on-line and in such a way that the changing levels of glutamate could be directly correlated to other temporal events such as change in heart rate or administration of a drug.



### 1.3 Microdialysis

The chosen method of *in vivo* sampling of glutamate was microdialysis. This technique, pioneered by Ungerstedt and Pycock (1974) has been well established as an effective method for both the sampling of neurochemicals and the delivery of drugs *in vivo*. There are a variety of microdialysis probe designs that operate on the same basic principles: a semi-permeable membrane is perfused with artificial cerebrospinal fluid (aCSF) by a small inlet tube. Neurochemicals present in the surrounding tissue diffuse across the membrane into the probe tip due to the concentration gradient. The aCSF leaving the probe tip via an outlet tube contains neurochemicals at concentrations representative of the concentrations in the surrounding tissue at the time the aCSF was in the probe tip. By perfusing the probe at a sufficiently low flow rate, the microdialysate (the perfusion fluid exiting the probe) can be assumed to have come to equilibrium with the surrounding tissue during its time in the probe tip.

### 1.4 Capillary Electrophoresis

Capillary electrophoresis (CE) is a powerful analytical technique that separates molecules based on their mobility through a buffer as determined by their charge to mass ratios. Among the chief advantages of CE are highly efficient separations, low separation times, low sample volumes, and simple column preparation.

Capillary electrophoresis employs a small internal diameter fused silica capillary. Coated with a polyimide coating, the capillary is strong and flexible. Treating the interior of the capillary with a strong base (figure 1.2) deprotonates the silanol groups of the interior wall, making the entire interior surface area a stationary phase of negative charges. When the capillary is perfused with a buffer solution the cations and anions in solution form a characteristic gradient. A layer of cations becomes more or less permanently associated with the negative charges of the interior wall, forming a stationary adsorbed layer. Inward from this layer is the diffuse layer, which is primarily composed of cations associating with the negative charge of the interior wall. Unlike the adsorbed layer, however, the diffuse layer is not stationary. The bulk of the fluid in the capillary is comprised of the remaining cations and anions. Although this characteristic gradient always forms, the net charge across the width of the capillary remains neutral.

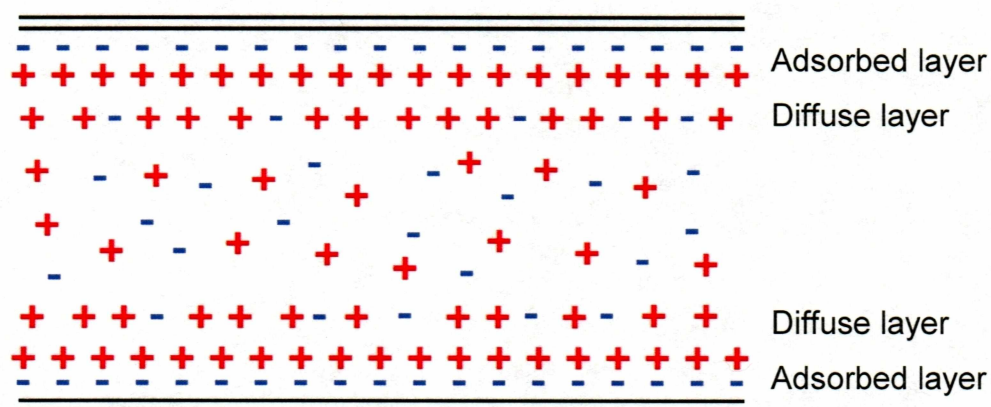


Figure 1.2 Side view of a conditioned electrophoresis capillary showing the characteristic charge gradient



When a potential is applied across the length of the capillary, the primarily positive diffuse layer migrates toward the negative cathode. This results in a bulk flow of fluid through the capillary, called electroendosmotic flow (EOF). When a sample is introduced onto the CE capillary, the EOF carries the sample plug toward the cathode. Electrically neutral molecules all migrate at the same rate as the EOF. Positively charged molecules are drawn more strongly toward the cathode in the direction of the EOF. Negatively charged molecules are drawn more strongly toward the anode, resisting the EOF. More massive charged molecules face more resistance when moving toward their preferred electrode, either with or against the bulk flow. Thus, charged molecules are separated by their charge to mass ratios ( $z/m$ ), the molecules with the highest  $z/m$  eluting first (figure 1.3).



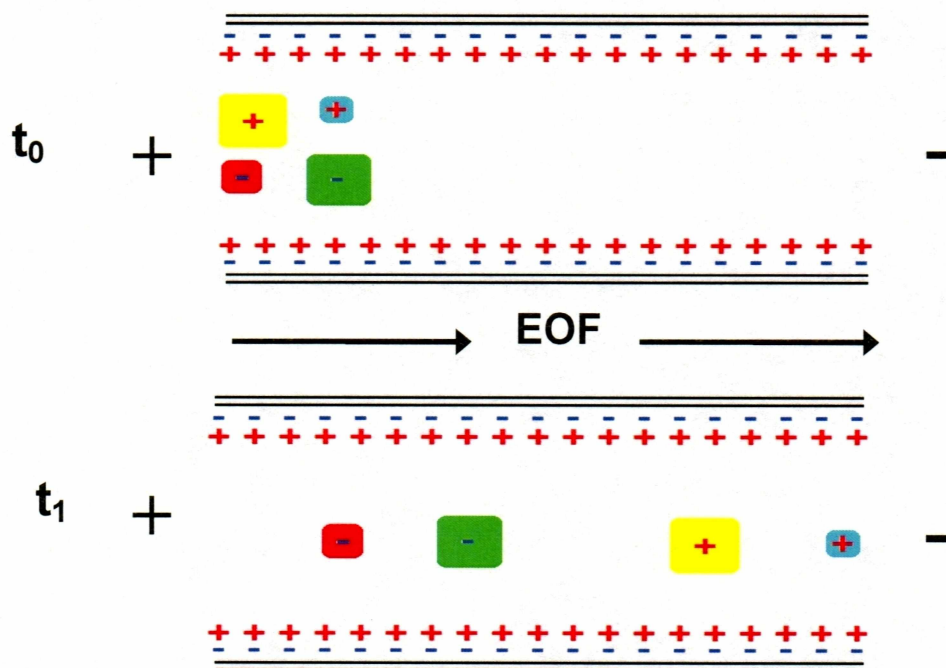


Figure 1.3 Separation of charged particles in capillary electrophoresis. Time  $t_0$ : the sample plug is a homogeneous mixture of component particles. Time  $t_1$ : As the sample migrates toward the negatively charged cathode, charged particles separate by their respective charge to mass ratios ( $z/m$ ).

## Chapter 2 Methods

### 2.1 Instrument

Several laboratories have described “home-built” CE/LIFD systems coupled with microdialysis. The system we built was based on the design used by Robert Kennedy at the University of Florida (Lada and Kennedy, 1997). In short, derivatizing reagents and aCSF eluting from a microdialysis probe combine and react in a capillary en route to injection onto the CE by flow-gated injection. Fluorescence is induced in derivatized analyte by a laser beam directed onto the capillary through a microscope objective. The resulting fluorescence is detected by a photomultiplier tube (PMT) and directed to a computer for analysis (figure 2.1)

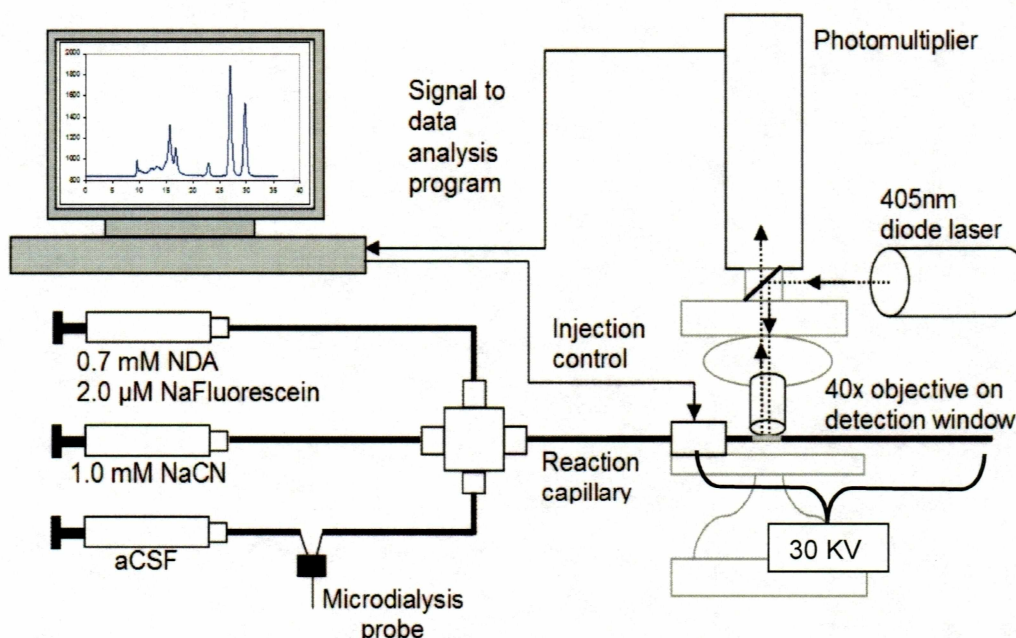


Figure 2.1 Schematic of the CE/LIFD system

### 2.1.1 Probe Construction

Microdialysis probes were constructed of two polyimide-coated fused silica capillaries (o.d.  $105\ \mu\text{m} \pm 4\ \mu\text{m}$ , i.d.  $40\ \mu\text{m} \pm 1\ \mu\text{m}$  depending on the batch) set side-by-side with a 1 mm offset at the tip. This tip was covered by a hollow fiber, semi-permeable cellulose membrane (figure 2.2). The inlet capillary was about 115 cm in length, the outlet about 125 cm.

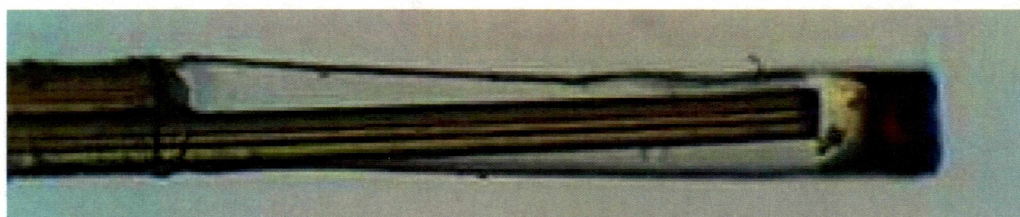


Figure 2.2 The tip of one of the microdialysis probes built in our laboratory. The offset of the two capillaries is about 1 mm.

Inlet and outlet capillaries were mated to their respective connections by HPLC fittings. The probes were mounted in push-pull connectors (Figure 2.3) for mating with guide cannulae surgically implanted in AGS. The probes were perfused with aCSF at  $0.1\ \mu\text{L}$  per minute.

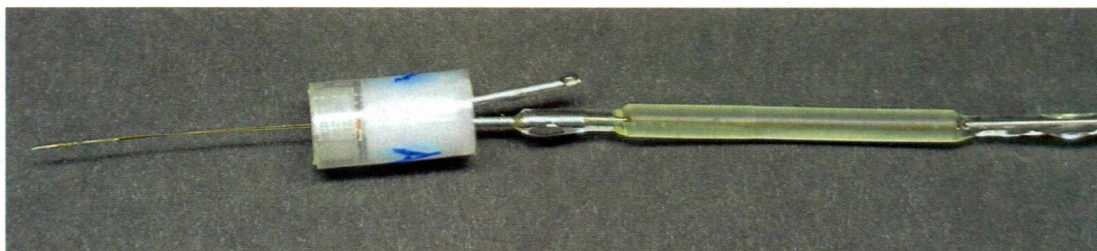


Figure 2.3 A fully assembled microdialysis probe featuring a push-pull connector and protective tygon tubing.



### 2.1.2 Derivatization

To achieve the detection limits necessary for *in vivo* concentrations of glutamate, it was necessary to derivatize the analytes with a fluorogenic agent (Figure 2.4). Naphthalene-2,3-dialdehyde (NDA) reacts with primary amines in the presence of cyanide to form fluorescent isoindoles (Carlson et al., 1986). The reaction proceeds most efficiently at pH 9.5 (De Montigny et al., 1987). The derivatized product has a  $\lambda_{\text{max}}$  at 420 nm and fluoresces at 490 nm (ibid.).

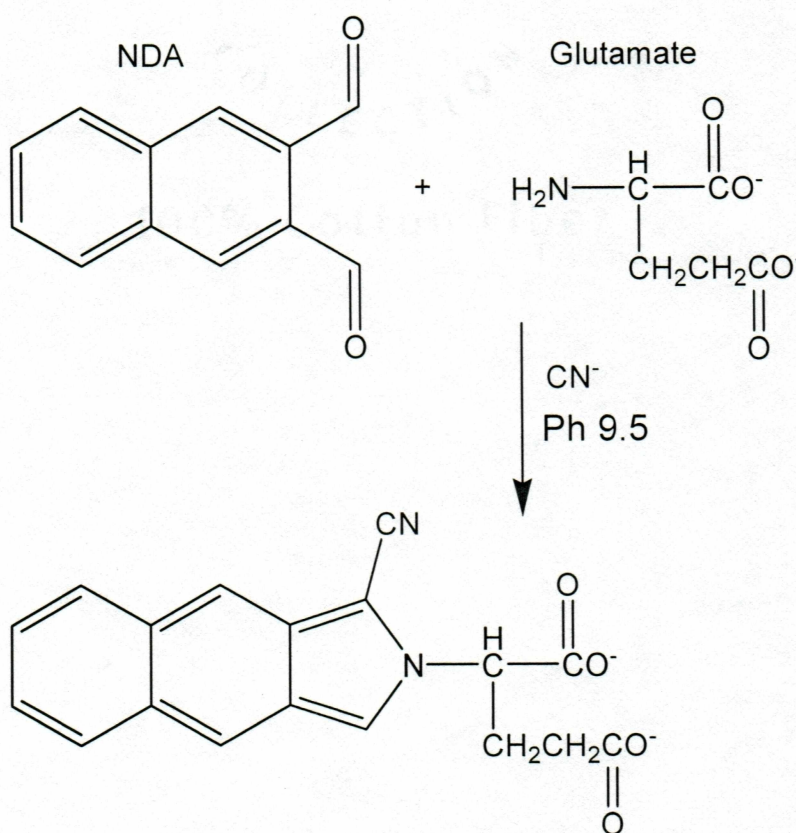


Figure 2.4 The derivatization reaction. In the presence of cyanide, NDA reacts with primary amines such as glutamate to form a fluorescent isoindole. Note that glutamate is a dianion, which gives it a lower  $z/m$  ratio than most other amino acids.



Derivatization of analytes was done on-column. Analyte-carrying microdialysate leaving the microdialysis probe entered a low-volume mixing T where it joined 0.7 mM NDA in 20%CH<sub>3</sub>CN and 1.0 mM NaCN in 60 mM sodium tetraborate decahydrate (pH 9.5) in a 75  $\mu$ m i.d mixing capillary. The retention time on the mixing capillary was 15 minutes to allow for complete derivatization of any primary amine neuromolecules present in the microdialysate.

### 2.1.3 Injection

On-line analysis of microdialysate was made possible by coupling the probe outlet to our CE system via flow-gated injection. The reaction capillary fed into an injection T (figure 2.4) where the majority of derivatized eluent was swept away by a cross flow buffer of 20 mM sodium tetraborate decahydrate (pH 9.5)

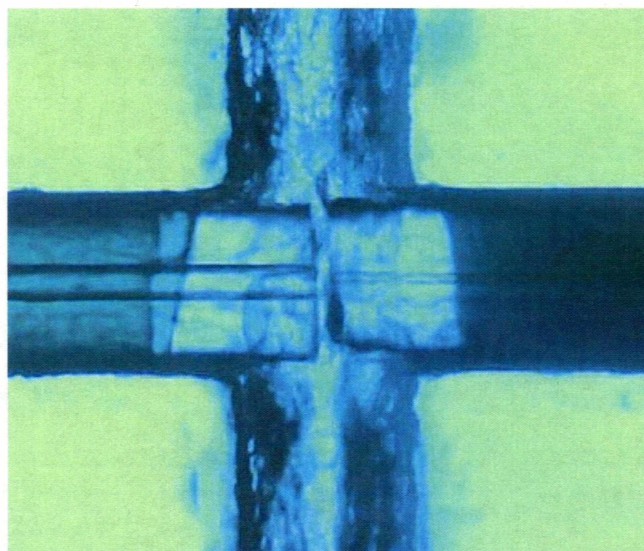


Figure 2.5 The flow-gated injection T. On the left is the 75  $\mu$ m i.d. reaction capillary. On the right is the 20  $\mu$ m i.d separation capillary. The gap between the two is about 40  $\mu$ m.

flowing through the injection T at 0.3 mL/min. The separation capillary was set in the injection T directly opposite the reaction capillary with an approximately 40  $\mu\text{m}$  gap between the two. The cross flow buffer acted as the run buffer, constantly supplying the separation capillary with fresh buffer. The cross flow buffer could be stopped for any desired amount of time by a computer-controlled solenoid. When the cross flow buffer was stopped, analyte would pool in the gap between the reaction and separation capillaries. Analyte would be drawn onto the separation capillary by EOF. To ensure baseline stability, a non-reactive fluorescent internal standard, sodium fluorescein, was added to the NDA solution at 2.00  $\mu\text{M}$  concentration.

#### 2.1.4 Separation

Separation of analyte was achieved by capillary electrophoresis on a fused silica glass capillary with an internal diameter of 20  $\mu\text{m}$ . The distance from the injection end of the separation capillary to the detection window was about 5.5 cm. The total length of the capillary was about 50 cm, the outlet of which was placed in a glass vial containing run buffer. A platinum electrode placed in the vial of buffer was the cathode of the circuit, and an alligator clip attached to the metal cross flow buffer outlet tube of the injection T was the anode. The voltage applied across the length of the capillary was 30 kV.



When preparing a new separation capillary, the capillary was flushed for 15 minutes each with 1.0 M NaOH, 0.1 M NaOH, and 20 mM sodium tetraborate decahydrate (pH 9.5). At the beginning of each day the separation capillary was reconditioned by flushing it for 5 minutes each with 0.1 M NaOH and 20 mM sodium tetraborate decahydrate (pH 9.5).

Glutamate was completely baseline resolved and eluted in 15-18 seconds. By overlapping injections (injecting a new sample before all of the analyte of the previous sample had eluted in order to decrease the time between samples) a new data point could be collected every 12-15 seconds.

#### 2.1.5 Detection

The separation capillary was mounted on special stage and affixed to the platform of a microscope (figure 2.5). About 5.5 cm downstream from the inlet end of the separation capillary, a section of the capillary was cleared of the protective polyimide coating to create a detection window. The beam of 405 nm diode laser was directed by a dichroic mirror and a 40x Olympus objective onto the detection window. When any potentially fluorescent molecule (including, but not limited to, any derivatized primary amine) passed through the illuminated section of capillary, its laser-induced fluorescence would be directed by the objective through the dichroic mirror to a PMT. The electronic signal of the PMT was interpreted by software as a peak.



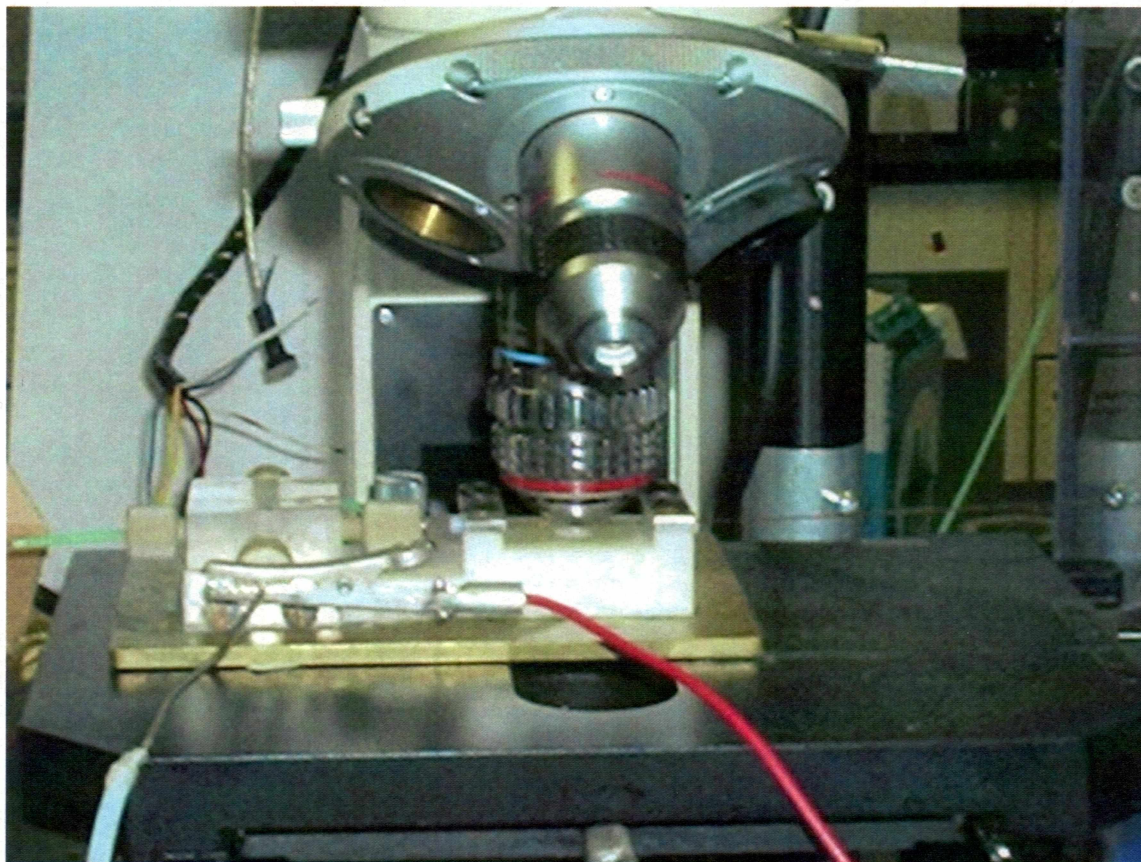


Figure 2.6 The mounted separation capillary. The microscope objective rests directly on top of a section of the separation capillary cleared of its polyimide coating. The separation capillary inlet is in the injection T, the clear plastic cube to the left of the objective. The alligator clip attached to the cross-flow buffer outlet is the anode of the electrophoretic circuit.

## 2.2 Data Collection and Analysis

Control of sample injection, interpretation of electronic data from the PMT, and integration of peaks from collected electropherograms were done with custom programs built to our specifications in Labview.



## 2.2.1 Data Acquisition

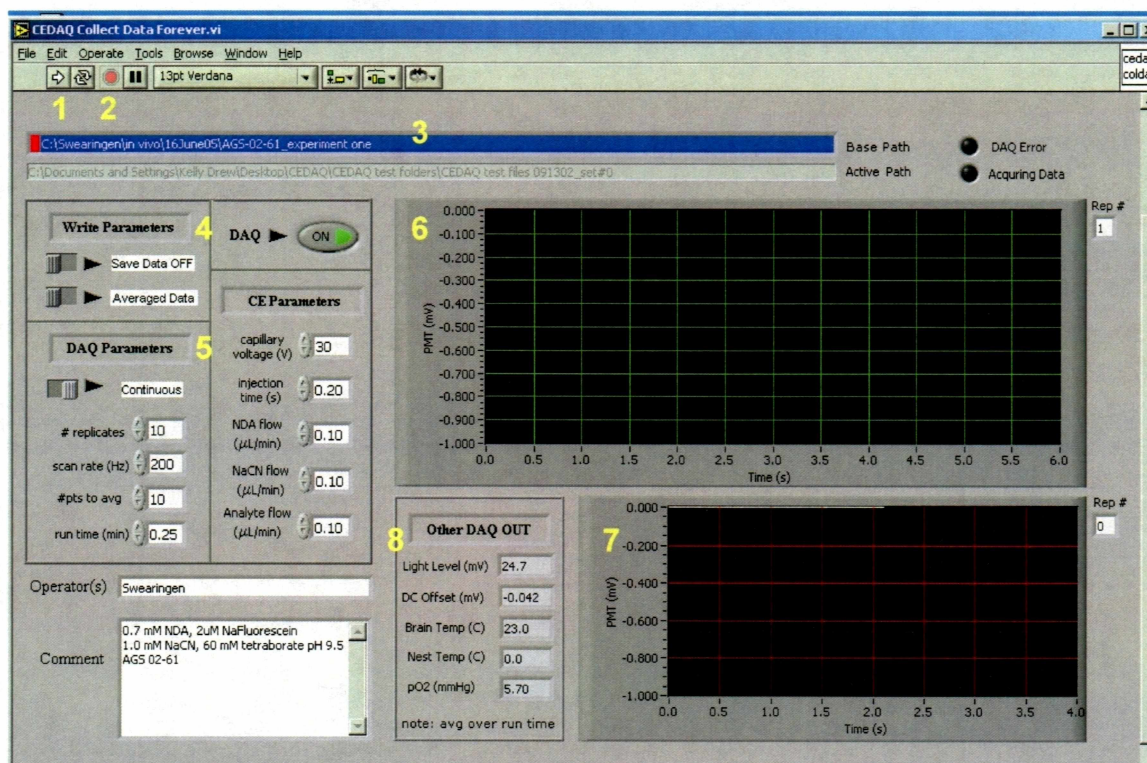


Figure 2.7 The instrument control and data acquisition screen

Injection time and data acquisition parameters were controlled from a computer using the visual interface shown in figure 2.7. 1) Initiates injection and data acquisition; 2) Stops data acquisition; 3) File path for saved data; 4) Write Parameters – the top switch toggles between Save Data OFF and Save Data On, the bottom switch toggles between “Averaged Data” and “All Data”; 5) DAQ Parameters – the switch toggles between “Finite” and “Continuous”, allowing the user to either collect a finite number of electropherograms or to continuously collect data sets containing as many electropherograms as are indicated in the “# replicates” window; 6) Signal output from the PMT appears in this window in real

time. The “Rep #” window to the upper right indicates which replicate number of the data set is being collected; 7) This window shows the previously collected electropherogram for reference; 8) These windows display real time data from various detectors that may be synchronously collecting data during an *in vivo* experiment.

## 2.2.2 Data viewer

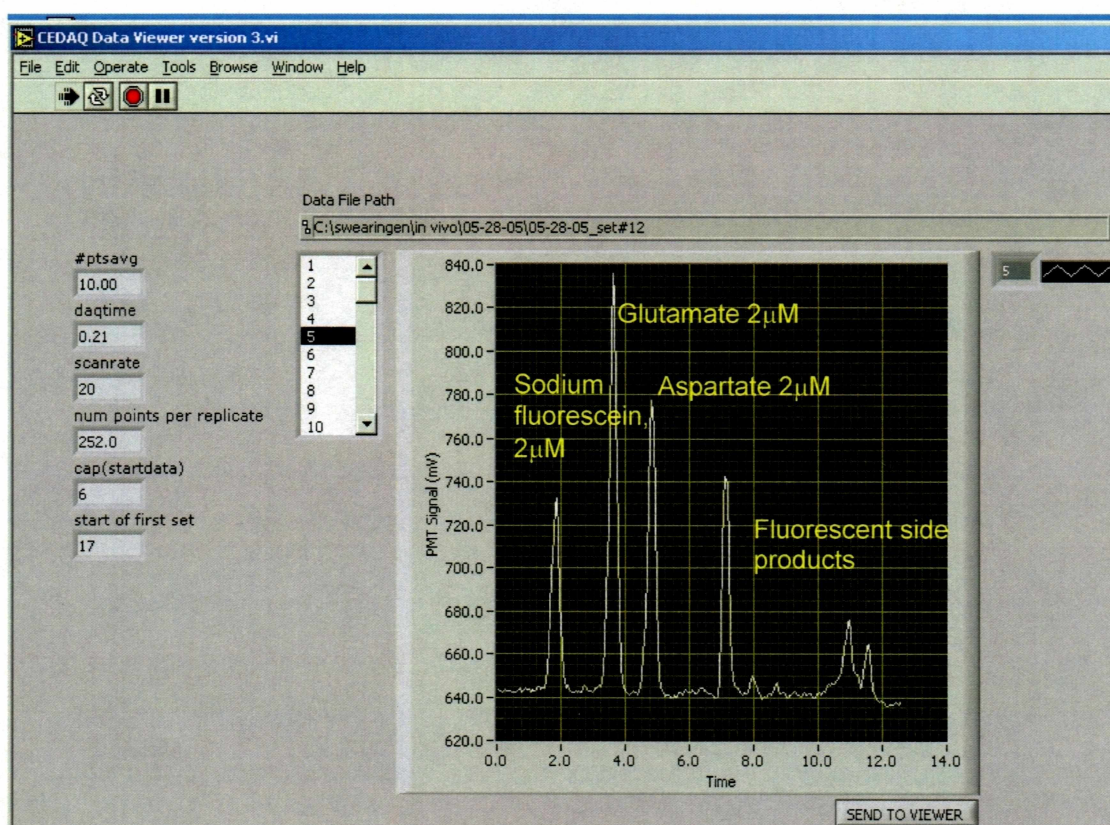


Figure 2.8 The data viewer screen. The component peaks of the electropherogram have been labeled.



The data viewer program allows the user to visually examine any saved set of electropherograms. The x and y scales can be adjusted to zoom in on any area of interest.

### 2.2.3 Peak integrator

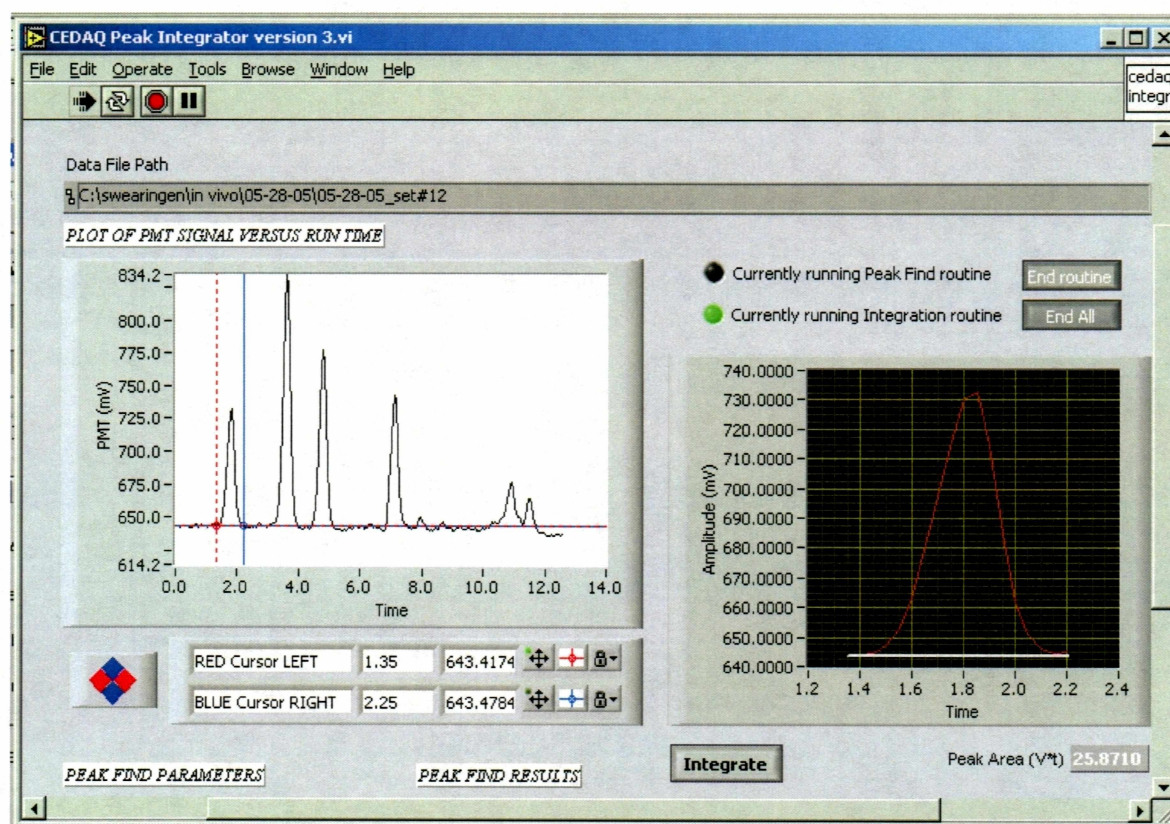


Figure 2.9 The peak integrator screen

The x and y scales of the view screen can be adjusted to zoom in on the area of interest. The red and blue lines are set on either side of the peak of interest and the area under the curve is given. The electropherograms in each data set were individually opened in the peak integrator program and the area found for the glutamate and sodium fluorescein peaks.



## 2.3 Calibration

Prior to *in vivo* analysis, the system was calibrated *in vitro* by collection of a 4-point calibration curve using sterile solutions of 2.0  $\mu\text{M}$ , 1.0  $\mu\text{M}$ , and 0.5  $\mu\text{M}$  glutamate in aCSF, as well as clean aCSF as a blank. Since the system collects data on-line, calibration data was collected simply by placing the tip of the probe for known amounts of time into vials containing the calibration solutions and recording the instrumental response.

## 2.4 *In vivo* methods

The probe and all parts of the instrument and apparatus that the aCSF came into contact with before entering the squirrel's brain had to be kept sterile. Syringes, tubing, and the probe were gas sterilized by ethylene oxide. Glass and plastic containers and pipette tips for solutions were sterilized by autoclave. Solutions were sterilized by filtering with 0.2  $\mu\text{m}$  filters. All sterile components were assembled under sterile conditions.

The subject animal was anesthetized with Halothane. While under anesthesia, the animal was fitted with a harness and the probe was inserted into the guide cannula. The animal was placed in a glass bowl on a motion-sensing rotor that allowed the animal to move freely without twisting up the probe tubing. *In vivo* data collection was begun immediately upon insertion of the probe.



## Chapter 3 Data

### 3.1 Probe Characterization

Microdialysis probes built as described above were tested *in vitro*.

Despite the small internal volume of the probes, a certain amount of mixing appeared to take place. This mixing was reflected as a gradual change in instrumental output after a discrete change in concentration at the probe. When the probe was changed from one calibration standard to another, an operation that took less than 5 seconds, it took about a minute for the change to be reflected by the instrument (figure 3.1). This was the limiting factor for temporal resolution of this technique.

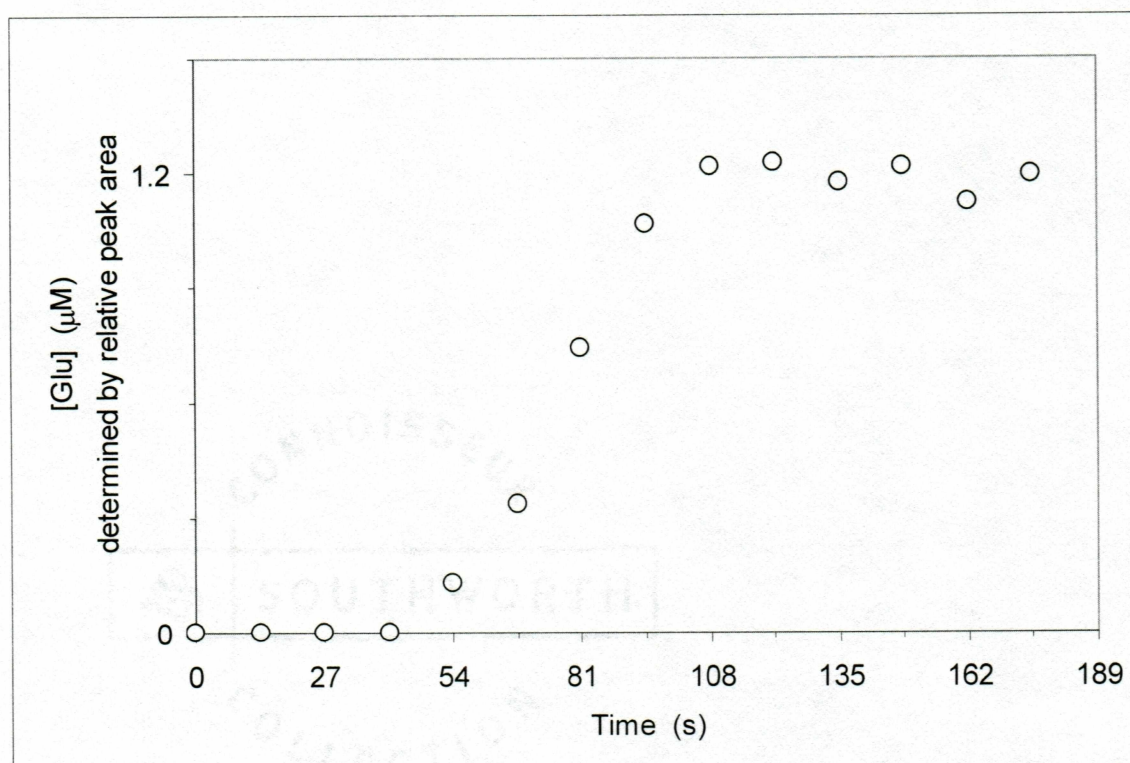


Figure 3.1 A discrete change in glutamate concentration is reflected in about one minute.

### 3.2 Calibration Data

Prior to each *in vivo* experiment, the system was calibrated with glutamate standards of 0.5  $\mu\text{M}$ , 1.0  $\mu\text{M}$ , and 2.0  $\mu\text{M}$  in aCSF (figure 3.2).

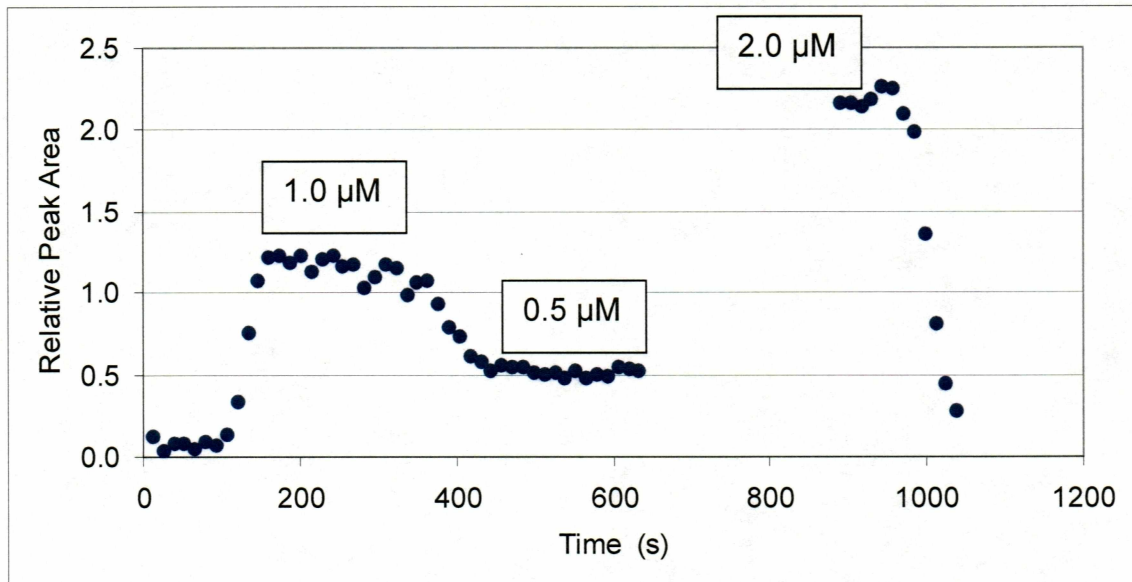


Figure 3.2 Calibration data for glutamate. The data are labeled with corresponding glutamate concentrations. At time 0, the probe is in aCSF with no glutamate added. No data was collected for a portion of the calibration experiment due to an air bubble that caused a temporary loss of current.

Calibration data showed the detection of glutamate to be linear over the range of 0.0  $\mu\text{M}$  to 2.0  $\mu\text{M}$ , the range in which *in vivo* concentrations of the neurotransmitter are expected to lie (figure 3.3).



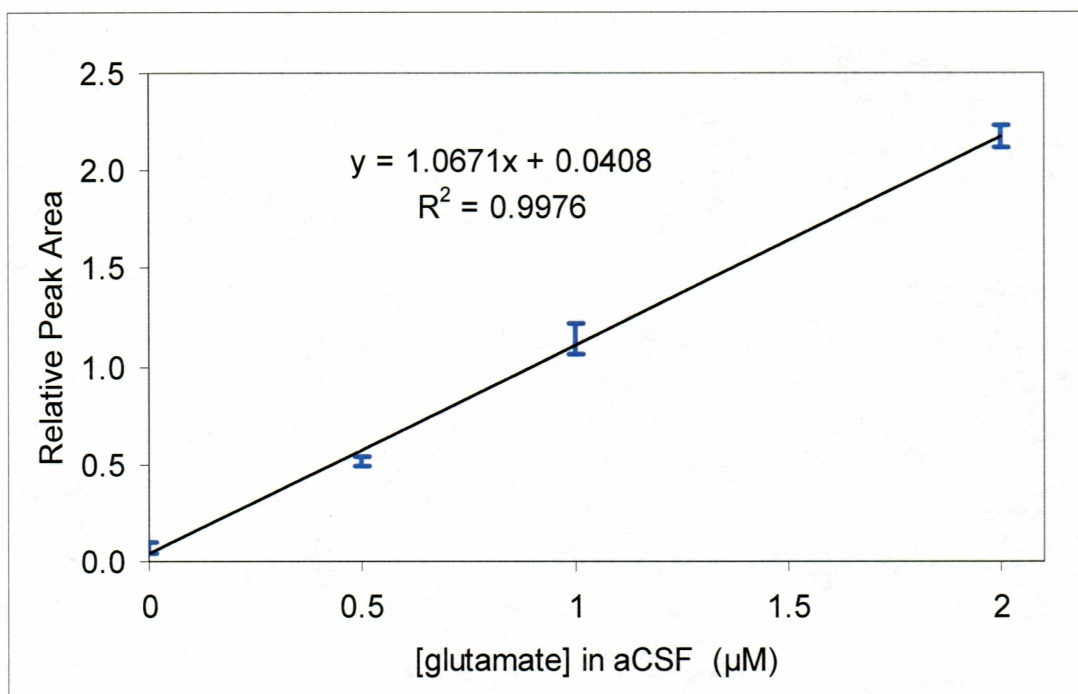


Figure 3.3 A calibration curve plotted with the data from Figure 3.2

### 3.3 *In vivo* data

An *in vivo* experiment was carried out to verify that baseline levels of glutamate could be detected. After obtaining a calibration curve, we attempted to insert the probe into the guide cannula of an arctic ground squirrel. However, we were unable to fit the probe through the guide cannula. After several attempts, the membrane of the probe was ruined. Supposing that the problem was that the wet probe membrane was swollen and unable to fit through the guide cannula, a new sterile probe was affixed in its place and inserted into the animal without first performing a calibration curve. (This problem has not been encountered in subsequent experiments, so the standard operating procedure still calls for

calibration of the system with the probe to be used prior to each new *in vivo* experiment.)

Figure 3.4 is a sample electropherogram from the data set collected. Based on previous calibrations, the glutamate peak is estimated to correspond to a glutamate concentration of 0.2  $\mu\text{M}$ .

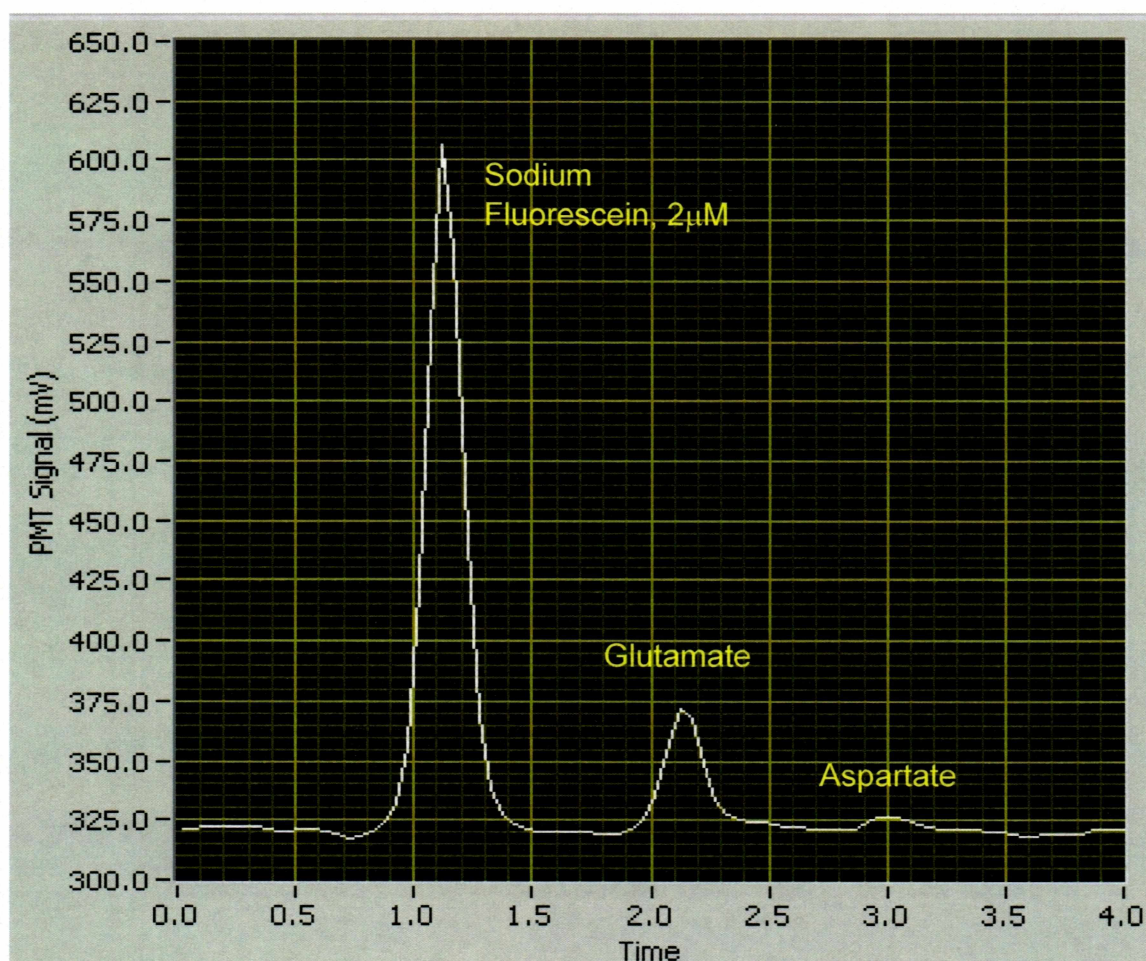


Figure 3.4 Detail of *in vivo* electropherogram.



## Chapter 4 Discussion

### 4.1 Analysis of the Technique

An instrument has been developed for on-line detection of glutamate *in vivo*. The instrument couples microdialysis to capillary electrophoresis by flow-gated injection. The system employs on-column derivatization of primary amines by NDA and cyanide for on-line detection by laser-induced fluorescence.

The microdialysis probes used have been shown to allow for quantitative detection of glutamate. Discrete changes in concentration *in vitro* are fully reflected instrumentally in about 1 minute. This is the limiting factor for temporal resolution of synaptic events.

Capillary electrophoresis has been shown to be an effective and efficient method for rapid separation of analytes; glutamate is separated in 12-15 seconds. The short run times ensure that frequency of sampling will not be a limiting factor in temporal resolution of experiments monitoring changing levels of glutamate.

Detection by laser-induced fluorescence allows detection of glutamate at the levels encountered *in vivo*. Derivatizing analyte on-column allows on-line detection of glutamate *in vivo*.

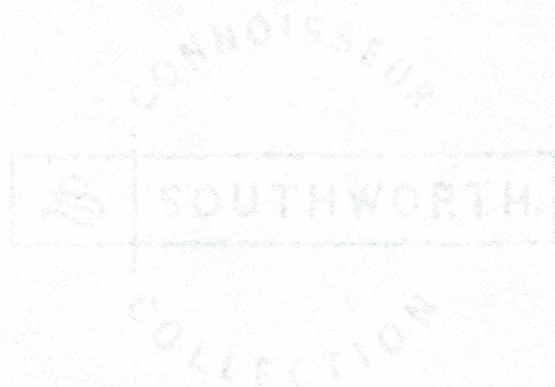
Protocols and standard operating procedures have been developed for assembly, running, and maintenance of the instrument. Sterile protocols have been developed for preparation for and execution of *in vivo* experiments with awake arctic ground squirrels.

#### 4.2 Future Work

While it has been shown that this instrument is capable detecting glutamate *in vivo*, it has yet to be demonstrated that the instrument will be capable of long-term monitoring of a ground squirrel entering and emerging from hibernation. The technique works well over periods of several hours, but we have not yet been able to demonstrate the sort of stability that will be needed for such a long-term experiment. The two greatest sources of error in this regard are: mechanical problems, such as inconsistent crossflow buffer flow rates and the microscope going out of focus; and chemical problems, such as maintaining optimal conditions on the separation capillary. The mechanical problems can be more easily addressed than the chemical problems. With our current set up, it is difficult or impossible to regularly recondition the separation capillary without disturbing any number of sensitive instrument parameters. Once the probe is inserted into an animal, there is no way to remove it and recalibrate the system, so it is vitally important that the system not be disturbed once an *in vivo* experiment is begun. This limitation will need to be addressed before the system can be used for long-term hibernation experiments.



In the mean time, short-term *in vivo* experiments can be performed on awake animals. Future experiments will include observing the effect on glutamate levels of administration of a glutamate uptake inhibitor directly into the SCN via microdialysis.



• 100% Cotton Fiber



### References

- Carlson RG, Srinivasachar K, Givens RS, Matuszewski BK New Derivatizing Agents for Amino Acids and Peptides. 1. Facile Synthesis of N-Substituted 1-cyanobenz[f]isoindoles and Their Spectroscopic Properties. *J. Org. Chem.* **1986**, 51(21), 3978
- De Montigny P, Stobaugh JF, Givens RS, Carlson RG, Srinivasachar K, Sternson LA, Higuchi T Napthalene-2,3-Dicarboxaldehyde/Cyanide Ion: A Rationally Designed Fluorogenic Reagent for Primary Amines. *Anal. Chem.* **1987**, 59(8), 1096
- Drew KL, Rice ME, Kuhn TB, Smith MA Neuroprotective Adaptations in Hibernation: Therapeutic Implications for Ischemia-Reperfusion, Traumatic Brain Injury and Neurodegenerative Diseases. *Free Radical Biology & Medicine* **2001**, 31(5), 563
- Harris MB, Milsom WK. Is Hibernation Facilitated by an Inhibition of Arousal? *Life in the Cold* (G Heldmaier and M Klingenspor; Eds) **2000**, 241
- Kilduff TS, Radeke CM, Randall TL, Sharp FR, Heller HC Suprachiasmatic Nucleus: Phase-Dependent Activation During the Hibernation Cycle. *Am. J. Physiol.* **1989**, 257, R605
- Lada MW, Kennedy RT High Temporal Resolution Monitoring of Glutamate and Aspartate *In Vivo* Using Microdialysis On-Line With Capillary Electrophoresis With Laser-Induced Fluorescence Detection. *Anal. Chem.* **1997**, 169(22), 4560
- Nurnberger F, Zhang Q, Pleschka K Neuropeptides and Neurotransmitters in the Suprachiasmatic Nucleus: Relationship With the Hibernation Process. *Life in the Cold* (G Heldmaier and M Klingenspor; Eds) **2000**
- Ruby NF, Dark J, Heller HC, Zucker I Ablation of Suprachiasmatic Nucleus Alters Timing of Hibernation in Ground Squirrels. *Proc. Natl. Acad. Sci. USA* **1996**, 93, 9864
- Sibson NR, Dhankhar A, Mason GF, Rothman DL, Behar KL, Shulman RG Stoichiometric Coupling of Brain Glucose Metabolism and Glutamatergic Neuronal Activity. *Proc. Natl. Acad. Sci. USA* **1998**, 95, 316-321
- Ungerstedt U, Pycock C Functional Correlates of Dopamine Neurotransmission. *Bul. Schweiz. Akad. Wiss.* **1974**, 30(1-3), 44